Exact and Gerchberg-Saxton solutions of the one-dimensional Pauli problem with Gaussian probability densities

Murillo R. Silva [*] and Alexys Bruno-Alfonso [†]

Department of Mathematics, UNESP - São Paulo State University, Bauru, SP, 17033-360, Brazil

The exact phase of one-dimensional quantum states with given Gaussian probability densities in the position and momentum representations is retrieved. The number of Pauli partners that are found depends on whether the Heisenberg uncertainty relation for position and momentum is saturated or not. Without saturation, two Pauli partners are found. They differ in the sign of the time derivative of their position uncertainties. The same problem is solved by an exact implementation of the Gerchberg-Saxton algorithm. Its convergence depends on uncertainty saturation as well.

I. INTRODUCTION

In 1933, Pauli remarked on the lack of a mathematical answer to whether knowledge of the probability densities in position and momentum representations defines a quantum state uniquely [1]. This is the same as to ask if all yields of the wave-function retrieval are necessarily linearly dependent. In general, the answer is negative. Linearly independent solutions called Pauli partners or Pauli pairs [2–6] have been reported for certain classes of probability densities [7]. The ongoing research on the Pauli problem has delved into (i) nonuniqueness [7–10], (ii) exact phase retrieval [11–13], (iii) numerical phase retrieval [5], and (iv) extensions of the problem [3,14,15]. One such extension with profound impact on modern physics and technology is quantum tomography [16,17]. It consists of identifying a mixed state of a quantum ensemble from a given set of measurements and plays a crucial role in the emerging quantum information technologies [18–20].

Phase-retrieval algorithms have been developed in several research areas beyond quantum mechanics. In 1972, Gerchberg and Saxton proposed an iterative procedure to retrieve the phase from image and diffraction pictures [21]. The algorithm and its improved versions [22] have been applied in classical optics [23–26], quantum optics [11,27,28], microscopy [29,30], control of coherent phonons [24], Raman spectroscopy [31], astronomy [32], and image encryption [33]. Optimization approaches to the phase-retrieval problem have been investigated as well [32,34].

The present work deals with the one-dimensional (1D) Pauli problem and has two main goals. The first one is to find exact solutions to the Pauli problem for the particular case where the probability densities in position and momentum representations have Gaussian shapes. This choice has motivations in semiclassical descriptions of a particle motion

[35] as well as in its mathematical simplicity. For instance, the quantum oscillator with initial Gaussian probability densities evolves, keeping the shape while changing geometric parameters such as center and spread [36,37]. The second goal is to investigate the convergence of the Gerchberg-Saxton algorithm (GSA), by performing exact calculations for each iteration. This should serve in test cases of numerical implementations of the algorithm, and should add to the present understanding of it.

The two goals are intertwined both mathematically and historically. On one hand, the exact solution allows a direct assessment of the accuracy of each GSA approximation. Equations obtained in the way towards the first goal are subsequently used to deal with the exact implementation of the GSA. On the other hand, our research started by numerically solving the Pauli problem through the GSA. Several numerical tests for the Gaussian probability densities seemingly produced parabolic profiles. This conjecture was proven by the exact implementation of the GSA. Then we realized that exact solutions can be obtained without iterative calculations.

The paper is organized as follows. Section II poses the Pauli problem for the case of Gaussian probability densities in position and momentum representations, and discusses candidates as Pauli partners. Section III solves the Pauli problem exactly, while Sec. IV describes the exact implementation of the Gerchberg-Saxton algorithm. Our main findings are summarized in Sec. V.

II. PAULI PROBLEM

We deal with the 1D quantum states of a particle of finite mass m. The Pauli problem is posed for a fixed time, and time dependence of the wave function is omitted. The phase retrieval does not depend on the Hamiltonian. However, to better analyze the Pauli partners, we consider a potential $V(x)$ and the Hamiltonian

$$\hat{H} = -\frac{\hbar^2}{2m}\frac{d^2}{dx^2} + V(x). \tag{1}$$

*murillo.silva@unesp.br
†alexys.bruno-alfonso@unesp.br

012210-1

The position and momentum representations of each quantum state, denoted by $\psi(x)$ and $\phi(k)$, bear a one-to-one relation given by the Fourier transforms

$$\phi(k) = \frac{1}{\sqrt{2\pi}} \int_{-\infty}^{+\infty} \psi(x) e^{-ikx} \, dx \quad (2)$$

and

$$\psi(x) = \frac{1}{\sqrt{2\pi}} \int_{-\infty}^{+\infty} \phi(k) e^{ikx} \, dk. \quad (3)$$

We give the momentum in units of the reduced Planck constant, i.e., $k = p/\hbar$, where p is the linear momentum.

The Pauli problem [38] asks for the phases $\theta(x)$ and $\eta(k)$ of $\psi(x)$ and $\phi(k)$, respectively, for given probability densities $|\psi(x)|^2$ and $|\phi(k)|^2$. We consider Gaussian densities in position and momentum representations, namely

$$|\psi(x)|^2 = \frac{1}{\sqrt{2\pi}\,\sigma_x} e^{-(x-x_0)^2/(2\sigma_x^2)} \quad (4)$$

and

$$|\phi(k)|^2 = \frac{1}{\sqrt{2\pi}\,\sigma_k} e^{-(k-k_0)^2/(2\sigma_k^2)}. \quad (5)$$

Here x_0 and k_0 are the expected values of position and momentum, respectively, whereas σ_x and σ_k are the standard deviations (uncertainties) of x and k, respectively.

Regarding nonuniqueness, we note that the probability densities in Eqs. (4) and (5) are symmetric with respect to $x = x_0$ and $k = k_0$, respectively, i.e.,

$$|\psi(2x_0 - x)| = |\psi(x)| \quad (6)$$

and

$$|\phi(2k_0 - k)| = |\phi(k)|. \quad (7)$$

According to Eq. (2), $\exp(-2ikx_0)\phi^*(k)$ is the Fourier transform of $\psi^*(2x_0 - x)$. Under Eq. (6), $\psi^*(2x_0 - x)$ either represents the same state as or is a Pauli partner of $\psi(x)$ [2–4,6,8]. Similarly, from Eq. (3), $\exp(2ik_0x)\psi^*(x)$ is the inverse Fourier transform of $\phi^*(2k_0 - k)$. Subject to Eq. (7), $\exp(2ik_0x)\psi^*(x)$ either represents the same state as or is a Pauli partner of $\psi(x)$. Combining the two mirror symmetries, the wave functions $\exp[2ik_0(x-x_0)]\psi(2x_0 - x)$ and $\exp[-2ix_0(k-k_0)]\phi(2k_0 - k)$ solve the same Pauli problem. This gives three candidates as Pauli partners when both probability densities are symmetric.

III. EXACT SOLUTIONS

We should find the phases $\theta(x)$ and $\eta(k)$ such that $\psi(x)$ and $\phi(k)$ satisfy Eqs. (2) to (5), namely

$$\psi(x) = \frac{1}{\sqrt[4]{2\pi}\,\sqrt{\sigma_x}} e^{i\theta(x)-(x-x_0)^2/(4\sigma_x^2)} \quad (8)$$

and

$$\phi(k) = \frac{1}{\sqrt[4]{(2\pi)^3}\,\sqrt{\sigma_x}} \int_{-\infty}^{+\infty} e^{i[\theta(x)-kx]-(x-x_0)^2/(4\sigma_x^2)} \, dx$$

$$= \frac{1}{\sqrt[4]{2\pi}\,\sqrt{\sigma_k}} e^{i\eta(k)-(k-k_0)^2/(4\sigma_k^2)}. \quad (9)$$

We make the parabolic ansatz

$$\theta(x) = a(x - x_0)^2 + b(x - x_0) + c, \quad (10)$$

where coefficients a, b, and c are unknown real constants. When $a = 0$ the curve degenerates into a straight line. Using Formula 3.323.2 of Ref. [39], we get

$$I(\alpha, \beta) = \int_{-\infty}^{+\infty} e^{-\alpha x^2 + i\beta x} \, dx = \sqrt{\frac{\pi}{\alpha}}\, e^{-\beta^2/(4\alpha)}, \quad (11)$$

where α and β are complex parameters with $\text{Re}\,(\alpha) > 0$. Moreover, the square root has positive real part. This leads to

$$\phi(k) = \frac{e^{i(c-kx_0)}}{\sqrt[4]{(2\pi)^3}\,\sqrt{\sigma_x}} I(\alpha, b - k)$$

$$= \frac{1}{\sqrt{2\alpha\,\sigma_x\,\sqrt{2\pi}}} \exp\left(i(c-kx_0) - \frac{(k-b)^2}{4\alpha}\right), \quad (12)$$

with $\alpha = (2\sigma_x)^{-2} - ia$.

By equating the absolute values of the second lines in Eqs. (9) and (12) we get

$$b = k_0 \quad (13)$$

and

$$\sigma_k = 2\sigma_x|\alpha| = 2\sigma_x\sqrt{\frac{1}{16\sigma_x^4} + a^2}. \quad (14)$$

Since a^2 cannot be negative, the problem is solvable when the Heisenberg uncertainty relation $\sigma_x\sigma_k \geqslant 1/2$ holds. Solving Eq. (14) we get

$$a = \pm\frac{\sqrt{\hbar - 1}}{4\sigma_x^2}, \quad (15)$$

where

$$\hbar = (2\sigma_x\sigma_k)^2. \quad (16)$$

The calligraphic symbol $\hbar$, mnemonic for Heisenberg, is a dimensionless parameter. The uncertainty relation reads $\hbar \geqslant 1$. It is said to be saturated when $\hbar = 1$.

Regarding $\eta(k)$, we use Eqs. (9) and (12) to obtain

$$\exp[i\eta(k)]$$

$$= \sqrt{\frac{|\alpha|}{\alpha}} \exp\left(i(c - kx_0) + \frac{i\,\text{Im}\,(\alpha)(k-k_0)^2}{4|\alpha|^2}\right). \quad (17)$$

Therefore, the momentum phase can be written as

$$\eta(k) = \bar{a}(k - k_0)^2 + \bar{b}(k - k_0) + \bar{c}, \quad (18)$$

with

$$\bar{a} = \frac{\text{Im}\,(\alpha)}{4|\alpha|^2} = -\frac{a\sigma_x^2}{\sigma_k^2} = \mp\frac{\sqrt{\hbar - 1}}{4\sigma_k^2}, \quad (19)$$

$$\bar{b} = -x_0, \quad (20)$$

and

$$\bar{c} = c - k_0 x_0 \pm \tfrac{1}{2}\arctan\sqrt{\hbar - 1}. \quad (21)$$

Since c can be chosen arbitrarily without affecting the quantum state, we take $c = 0$. Anyway, as shown in Eq. (15),

the Pauli problem under investigation lacks uniqueness when $\hbar > 1$. The two choices for the sign of a lead to a couple of Pauli partners [2–4,6]. They are linearly independent, since

$$\psi_-(x) = \exp\left[-\frac{i\sqrt{\hbar-1}}{2}\left(\frac{x-x_0}{\sigma_x}\right)^2\right]\psi_+(x). \qquad (22)$$

The density of probability current associated with the Hamiltonian in Eq. (1) is given by

$$j(x) = \frac{\hbar}{m}\,\mathrm{Im}\,[\psi^*(x)\psi'(x)] = \frac{\hbar|\psi(x)|^2\theta'(x)}{m}$$
$$= \frac{\hbar|\psi(x)|^2}{m}[2a(x-x_0)+k_0]. \qquad (23)$$

This is affected by the sign of a in Eq. (15).

Differences between the partners are more apparent in terms of the velocity field that multiplies the probability density in Eq. (23), i.e.,

$$v(x) = \frac{\hbar}{m}[2a(x-x_0)+k_0]. \qquad (24)$$

This is a superposition of a uniform and a linearly varying field. For the partner with positive a, the latter field represents positive speed for $x > x_0$ and negative speed for $x < x_0$. Then the position uncertainty increases with time, i.e., the wave packet is expanding. Similarly, the partner with $a < 0$ shrinks with time.

The time derivative of the position uncertainty σ_x can be obtained through the generalized Ehrenfest theorem [40]. For the wave function in Eq. (8) we get

$$\frac{d\sigma_x^2}{dt} = \frac{d}{dt}[\langle\psi|x^2|\psi\rangle - \langle\psi|x|\psi\rangle^2]$$
$$= \frac{\langle\psi|[x^2,\hat{p}^2/2m]|\psi\rangle}{i\hbar} - \frac{2\hbar x_0 k_0}{m}$$
$$= \frac{2\hbar a\sigma_x^2}{m} = 2\sigma_x\frac{d\sigma_x}{dt}, \qquad (25)$$

thus

$$\frac{d\sigma_x}{dt} = \frac{\hbar a\sigma_x}{m}. \qquad (26)$$

This gives the relation between the concavity of $\theta(x)$ and the time derivative of the position uncertainty.

Changes in momentum uncertainty will depend on the specific interaction potential $V(x)$, namely

$$\frac{d\sigma_k^2}{dt} = \frac{1}{\hbar^2}\frac{d}{dt}[\langle\psi|\hat{p}^2|\psi\rangle - \langle\psi|\hat{p}|\psi\rangle^2]$$
$$= \frac{\langle\psi|[\hat{p}^2,V(x)]|\psi\rangle}{i\hbar^3} + \frac{2\hbar k_0}{\hbar}\langle\psi|V'(x)|\psi\rangle$$
$$= \frac{2\hbar\bar{a}\sigma_k^2}{\hbar}\langle\psi|V''(x)|\psi\rangle = 2\sigma_k\frac{d\sigma_k}{dt}. \qquad (27)$$

i.e.,

$$\frac{d\sigma_k}{dt} = \frac{\bar{a}\sigma_k}{\hbar}\langle\psi|V''(x)|\psi\rangle. \qquad (28)$$

For the harmonic oscillator of frequency ω, with $V(x) = m\omega^2 x^2/2$, we have $V''(x) = m\omega^2$ and

$$\frac{d\sigma_k}{dt} = \frac{m\omega^2\bar{a}\sigma_k}{\hbar} = \frac{\hbar\bar{a}\sigma_k}{m\lambda^4}, \qquad (29)$$

where $\lambda = (m\omega/\hbar)^{-1/2}$ is the characteristic length. Since a and $\bar{a}$ have opposite signs, the position and momentum uncertainties have opposite time derivatives. Expansion in one representation means contraction in the other one. In fact, Eqs. (19), (26), and (29) lead to

$$\frac{\sigma_x\,d\sigma_x}{\lambda^2} + \lambda^2\sigma_k\,d\sigma_k = 0, \qquad (30)$$

which solves as

$$\frac{\sigma_x^2}{\lambda^2} + \lambda^2\sigma_k^2 = W, \qquad (31)$$

where W is a positive constant.

Considering the last paragraph of Sec. II, we can analyze the three candidates as Pauli partners of $\psi_+(x)$. Since the solutions can be written as

$$\psi_\pm(x) = |\psi(x)|\,e^{i[a_\pm(x-x_0)^2+k_0(x-x_0)]} \qquad (32)$$

and

$$\phi_\pm(k) = |\phi(k)|\,e^{i[\bar{a}_\pm(k-k_0)^2-x_0k+\frac{1}{2}\arctan(4\sigma_x^2 a_\pm)]} \qquad (33)$$

we have

$$\psi_+^*(2x_0-x) = \psi_-(x), \qquad (34a)$$
$$e^{-2ix_0k}\phi_+^*(k) = \phi_-(k), \qquad (34b)$$

$$e^{2ik_0x}\psi_+^*(x) = e^{2ik_0x_0}\psi_-(x), \qquad (35a)$$
$$\phi_+^*(2k_0-k) = e^{2ik_0x_0}\phi_-(k), \qquad (35b)$$

and

$$e^{2ik_0(x-x_0)}\psi_+(2x_0-x) = \psi_-(x), \qquad (36a)$$
$$e^{-2ix_0(k-k_0)}\phi_+(2k_0-k) = \phi_-(k). \qquad (36b)$$

It is seen that such candidates reduce to $\psi_-(x)$, disregarding nonphysical rigid phase shifts.

In the special case $\hbar = 1$ we get $a = \bar{a} = 0$. Then, Eqs. (10) and (18) degenerate into the straight lines $\theta(x) = k_0(x-x_0)$ and $\eta(k) = -x_0 k$, respectively. Moreover, we have $\psi_+(x) = \psi_-(x)$. Finding a single solution for the Pauli problem with saturated Heisenberg relation should come as no surprise. It is well known that uncertainty saturation with given values of x_0, k_0, and σ_x leads to a single quantum state represented by [40]

$$\psi(x) = \frac{1}{\sqrt[4]{2\pi}\,\sqrt{\sigma_x}}\exp\left(-\frac{(x-x_0)^2}{2\sigma_x^2}+ik_0x\right). \qquad (37)$$

We illustrate the analytical results by solving the Pauli problem given by Eqs. (4) and (5), with $x_0 = 2$, $\sigma_x = 1/2$, $k_0 = 3$, and $\sigma_k = \sqrt{5}/2$. The Heisenberg relation is fulfilled but not saturated, since $\hbar = 5/4 > 1$. The position is given in units of an arbitrary length denoted by λ. Correspondingly, the momentum k is given in units of λ^{-1}. The Gaussian profiles of absolute values of $|\psi(x)|$ and $|\phi(k)|$ are displayed in
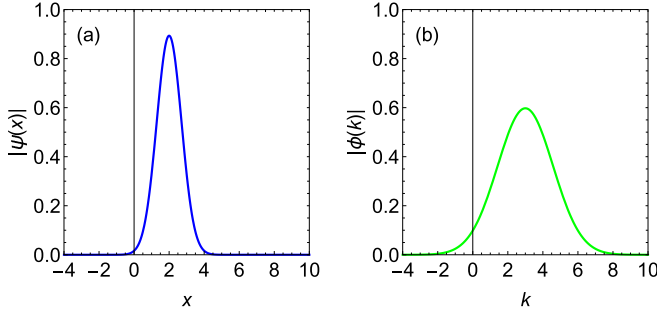
FIG. 1. Absolute values of (a) $\psi(x)$ and (b) $\phi(k)$, for $x_0 = 2$, $\sigma_x = 1/2$, $k_0 = 3$, and $\sigma_k = \sqrt{5}/2$. The position is given in units of an arbitrary length denoted by λ. Correspondingly, the momentum k is given in units of λ^{-1}. $|\psi(x)|$ and $|\phi(k)|$ are given in units of $\lambda^{-1/2}$ and $\lambda^{1/2}$, respectively.

Fig. 1. These functions are given in units of $\lambda^{-1/2}$ and $\lambda^{1/2}$, respectively.

From Eqs. (13), (15), (19), and (20) we obtain $b = 3$, $a = \pm 1/2$, $\bar{a} = \mp 1/10$, and $\bar{b} = -2$. Choosing $c = 0$, Eq. (21) leads to $\bar{c} = -6 \pm 0.5 \arctan(1/2)$. The parabolic phases of $\psi(x)$ and $\phi(k)$ for the Pauli partners are displayed in Fig. 2. In Fig. 2(a) the parabolas of different partners are tangent to each other at $(x, \theta) = (x_0, 0)$. The upward (downward) parabola is for $a > 0$ $(a < 0)$, i.e., the expanding (shrinking) partner. Their vertices are at $x = 2 \mp 3$, i.e., $x = -1$ and $x = 5$. In Fig. 2(b) the vertices are at $k = 3 \mp 10$, i.e., $k = -7$ and $k = 13$.

Figure 3 displays the real and imaginary parts of $\psi(x)$ for the Pauli partners that solve the problem of Fig. 1. It is apparent that

$$\mathrm{Re}\left[\psi_-(x_0 + \Delta x)\right] = \mathrm{Re}\left[\psi_+(x_0 - \Delta x)\right], \qquad (38a)$$

$$\mathrm{Im}\left[\psi_-(x_0 + \Delta x)\right] = -\mathrm{Im}\left[\psi_+(x_0 - \Delta x)\right] \qquad (38b)$$

hold in this case. This is equivalent to Eq. (34a).

Differences between the probability-current densities of the Pauli partners are seen in Fig. 4. Here $j_+(x)$ $[j_-(x)]$ correspond to the expanding (shrinking) Pauli partner, i.e., $a > 0$ $(a < 0)$. According to Eq. (34a), those currents are related by $j_-(x_0 + \Delta x) = j_+(x_0 - \Delta x)$.
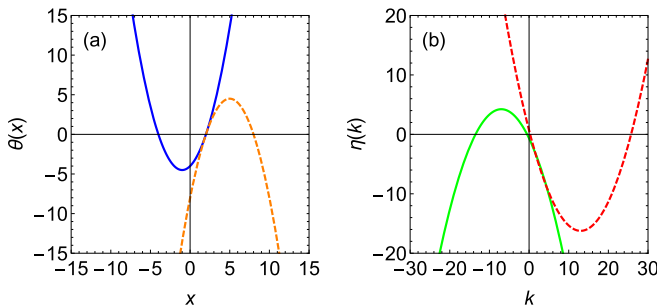

FIG. 2. The phases (a) $\theta(x)$ and (b) $\eta(k)$ that solve the Pauli problem with the Gaussian parameters of Fig. 1. The solid (dashed) lines are for the expanding (shrinking) Pauli partner.
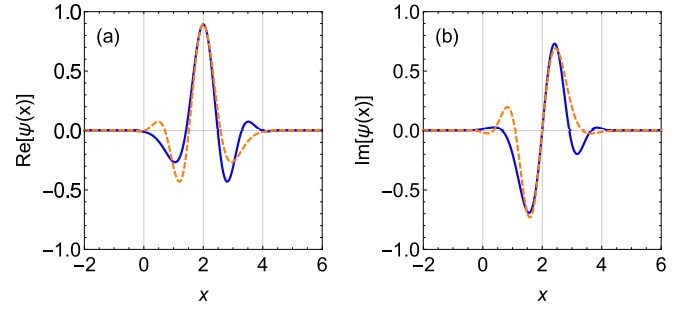
FIG. 3. (a) Real and (b) imaginary parts of $\psi(x)$, in units of $\lambda^{-1/2}$, for the Pauli partners of Fig. 2. The solid (dashed) lines are for the expanding (shrinking) partner.

IV. GERCHBERG-SAXTON ALGORITHM

Having exact solutions to the Pauli problem with Gaussian probability densities allows us to analyze the application of the GSA. This is an iterative procedure where an initial phase profile leads to a sequence of approximations that expectedly converges to one of the exact solutions. Our initial approximation for $\theta(x)$ will be an arbitrary straight line or parabolic profile, denoted by $\theta_0(x)$. According to Eq. (12), this guarantees that subsequent approximations denoted by $\theta_n(x)$ will be either a straight line or a parabola. In this way, convergence of the GSA can be investigated analytically.

Let us consider that at the nth iteration, with $n = 0, 1, 2, \ldots$, the approximation for $\theta(x)$ is given by

$$\theta_n(x) = a_n(x - x_0)^2 + b_n(x - x_0) + c_n. \qquad (39)$$

According to Eq. (12), Eq. (2) approximates $\phi(k)$ by

$$\phi_n(k) = \sqrt{\frac{\pi}{\frac{1}{4\sigma_x^2} - ia_n}} \frac{e^{i(c_n - kx_0) - \frac{(k - b_n)^2}{4\left(\frac{1}{4\sigma_x^2} - ia_n\right)}}}{\sqrt[4]{2\pi}\sqrt{\sigma_x}}. \qquad (40)$$

This implies

$$\eta_n(k) = \bar{a}_n(k - k_0)^2 + \bar{b}_n(k - k_0) + \bar{c}_n, \qquad (41)$$

where

$$\bar{a}_n = -\frac{a_n}{4\left(\frac{1}{16\sigma_x^4} + a_n^2\right)}, \qquad (42)$$

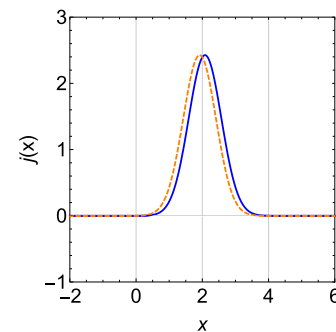$$\bar{b}_n = -[x_0 + 2\bar{a}_n(b_n - k_0)], \qquad (43)$$

FIG. 4. Probability currents, in units of $\hbar m^{-1}\lambda^{-2}$, for the Pauli partners of Fig. 2. The solid (dashed) line is for the expanding (shrinking) partner.

and

$$\bar{c}_n = \bar{a}_n(b_n - k_0)^2 + c_n - k_0x_0 + \frac{1}{2}\arctan\left(4a_n\sigma_x^2\right). \quad (44)$$

Now Eq. (3) gives the next approximation

$$\psi_{n+1}(x) = \sqrt{\frac{\pi}{\frac{1}{4\sigma_k^2} - i\bar{a}_n}} \frac{e^{i(\bar{c}_n + xk_0) - \frac{(x+\bar{b}_n)^2}{4\left(\frac{1}{4\sigma_k^2} - i\bar{a}_n\right)}}}{\sqrt[4]{2\pi}\sqrt{\sigma_k}}. \quad (45)$$

This yields a new approximation for $\theta(x)$ given by

$$\theta_{n+1}(x) = a_{n+1}(x - x_0)^2 + b_{n+1}(x - x_0) + c_{n+1}, \quad (46)$$

with

$$a_{n+1} = -\frac{\bar{a}_n}{4\left(\frac{1}{16\sigma_k^4} + \bar{a}_n^2\right)}, \quad (47)$$

$$b_{n+1} = k_0 + 2a_{n+1}(\bar{b}_n + x_0), \quad (48)$$

and

$$c_{n+1} = a_{n+1}(\bar{b}_n + x_0)^2 + \bar{c}_n + k_0x_0 + \frac{1}{2}\arctan\left(4\bar{a}_n\sigma_k^2\right). \quad (49)$$

We simplify the GSA by choosing $c_0 = 0$ and resetting c_n to zero at every iteration. This is consistent with our choice for the exact solution in Sec. III.

Putting Eqs. (42) and (43) into Eqs. (47) and (48) we obtain a direct relation between $\theta_n(x)$ and $\theta_{n+1}(x)$, i.e.,

$$a_{n+1} = \frac{a_n}{\frac{1}{\sigma_k^4}\left(\frac{1}{16\sigma_x^4} + a_n^2\right) + \frac{a_n^2}{\frac{1}{16\sigma_x^4} + a_n^2}} \quad (50)$$

and

$$b_{n+1} = k_0 + \frac{a_n a_{n+1}(b_n - k_0)}{\frac{1}{16\sigma_x^4} + a_n^2}. \quad (51)$$

The recurrence relations in Eqs. (50) and (51) set our exact implementation of the GSA. To analyze its convergence, we concentrate on the position representation. By introducing the sequence $q_n = a_n/\sigma_k^2$, we get

$$q_{n+1} = \frac{q_n}{\frac{1}{\hbar^2} + q_n^2 + \frac{q_n^2}{\frac{1}{\hbar^2} + q_n^2}} \quad (52)$$

and

$$b_{n+1} = k_0 + \frac{q_n q_{n+1}(b_n - k_0)}{\frac{1}{\hbar^2} + q_n^2}. \quad (53)$$

Choosing $q_0 = 0$ yields $q_n = 0$ for all n. This solves the Pauli problem in just one step, provided the Heisenberg relation is saturated ($\hbar = 1$). When $q_0 = 0$ and $\hbar > 1$, the procedure gets stuck to the straight line given by the first iteration. It is not able to choose either the upward or the downward parabola. If the calculations were done numerically, then symmetry could be broken by round-off errors, and evolution to one of the partners would occur.

Instead, $q_0 \neq 0$ guarantees q_n will not ever vanish. The algebra is simpler in terms of $u_n = 1/q_n$, namely

$$u_{n+1} = \frac{u_n}{\hbar^2} + \frac{1}{u_n} + \frac{1}{\frac{u_n}{\hbar^2} + \frac{1}{u_n}}$$

$$= 2 + \left(\sqrt{\frac{u_n}{\hbar^2} + \frac{1}{u_n}} - \sqrt{\frac{1}{\frac{u_n}{\hbar^2} + \frac{1}{u_n}}}\right)^2 \geqslant 2. \quad (54)$$

Since $u_0 \neq 0$, u_n does not change sign. We shall limit ourselves to the case $u_0 > 0$. The case $u_0 < 0$ can be analyzed by considering the sequence $(-u_n)$.

We will first prove that if $\hbar > 1$, then

$$\lim_{n\to\infty} u_n = u = \frac{\sigma_k^2}{a} = \frac{\hbar}{\sqrt{\hbar - 1}} \geqslant 2. \quad (55)$$

If the limit exists, Eq. (54), leads to

$$u = \frac{u}{\hbar^2} + \frac{1}{u} + \frac{1}{\frac{u}{\hbar^2} + \frac{1}{u}}, \quad (56)$$

whose positive solution is given by (55). To prove the existence, we note that the error $u_n - u$ obeys the recurrence relation

$$u_{n+1} - u = \frac{u_n}{\hbar^2} + \frac{1}{u_n} + \frac{1}{\frac{u_n}{\hbar^2} + \frac{1}{u_n}} - u$$

$$= r_n(u_n - u), \quad (57)$$

with

$$r_n = \frac{1}{\hbar^2} - \frac{1}{u_n u} + \frac{\hbar(\hbar - 1 - u_n/u)}{u_n^2 + \hbar^2}. \quad (58)$$

The sequence (u_n) converges exponentially or faster provided the ratio r_n is bounded by fixed numbers in the open interval $(-1, 1)$, for sufficiently large n. Since $\hbar > 1$, we have

$$r_n \leqslant \frac{1}{\hbar^2} + \frac{\hbar(\hbar - 1)}{u_n^2 + \hbar^2} \leqslant \frac{1}{\hbar^2} + \frac{\hbar - 1}{\hbar} = 1 - \frac{1}{u^2}. \quad (59)$$

On the other hand, for $n \geqslant 1$ we have $u_n \geqslant 2$ and

$$r_n \geqslant -\frac{1}{u u_n} - \frac{\hbar u_n/u}{u_n^2 + \hbar^2} \geqslant -\frac{1}{4} - \frac{1}{2u} \geqslant -\frac{1}{2}. \quad (60)$$

This proves that (u_n), (q_n), (a_n) converge at least exponentially. In turn, (b_n) converges exponentially to $b = k_0$ as given by

$$b_{n+1} - k_0 \approx \frac{(b_n - k_0)}{\frac{u^2}{\hbar^2} + 1} = \left(1 - \frac{1}{\hbar}\right)(b_n - k_0). \quad (61)$$

It is important to analyze the behavior of r_n as the GSA runs. From Eqs. (55) and (58), its limit is given by

$$r = \lim_{u_n\to u} r_n = \left(1 - \frac{2}{\hbar}\right)^2. \quad (62)$$

Figure 5 shows the limit ratio r as a function of $\hbar$. It is seen that $0 \leqslant r < 1$. The exponential decay is rather slow when r is near 1, i.e., $\hbar \approx 1$ or $\hbar \gg 1$. In contrast, convergence is very fast when $\hbar \approx 2$. In the special case $\hbar = 2$, corresponding to $u = 2$, the limit ratio r vanishes. The error $u_n - u$ will not vanish after a finite number of iterations. A Taylor expansion
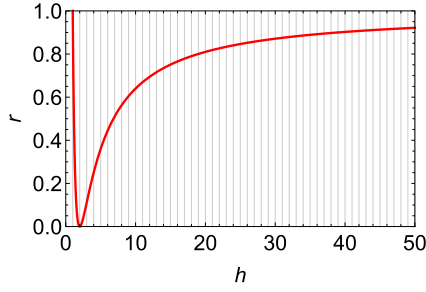
FIG. 5. The asymptotic value r of the ratio between consecutive errors $u_{n+1} - u$ and $u_n - u$ in the Gerchberg-Saxton algorithm, as a function of the dimensionless parameter $\hbar$.

of r_n in terms of u_n around $u = 2$ gives $r_n \approx (u_n - 2)^3/64$ and $u_{n+1} - 2 \approx (u_n - 2)^4/64$, thus

$$u_{n+m} - 2 \approx 4\left(\frac{u_n - 2}{4}\right)^{4^m}, \tag{63}$$

This is a double-exponential convergence [41], which is much faster than the exponential one.

The asymptotic behavior of (a_n) is given by

$$a_n - a \approx \frac{da}{du}(u_n - u) = -\frac{\sigma_k^2}{u^2}(u_n - u). \tag{64}$$

Hence we have $a_{n+1} - a \approx r(a_n - a)$, when $\hbar > 1$ and $\hbar \neq 2$, whereas $a_{n+1} - a \approx (a_n - a)^4/64$, for $\hbar = 2$. When $\hbar > 1$, (b_n) converges faster than (a_n) if and only if $1 - 1/\hbar < (1 - 2/\hbar)^2$, i.e., $\hbar < 4/3$.

Figure 6 shows the GSA results for the Pauli problem of Fig. 1, where $\hbar = 5/4$. The solid lines are for the exact solution of Fig. 2(a). The dashed line in Fig. 6(a) displays the initial profile $\theta_0(x)$ for $a_0 = 1/6$ and $b_0 = -3/2$. The dashed lines in the remaining panels of Fig. 6 correspond to $\theta_n(x)$ for the first seven GSA iterations. Fast convergence of $\theta_n(x)$ to the exact profile $\theta(x)$ is apparent. For sufficiently large n, a_n, and b_n converge exponentially with their errors shrinking by factors near $r = 0.36$ and $1 - \hbar^{-1} = 0.2$, respectively.

A faster convergence of (a_n) is displayed in Fig. 7, where the Gaussian parameters of the Pauli problem are $x_0 = 2$, $\sigma_x = 1/2$, $k_0 = 3$, and $\sigma_k = \sqrt{2}$. These values lead to $\hbar = 2$, and the exact solution is given by $a = \sigma_k^2/2 = 1$ and $b = k_0 = 3$. The initial approximation in Fig. 7(a) is the same as of Fig. 6(a). The remaining panels of Fig. 7 correspond to $\theta_n(x)$ for the first five GSA iterations. The sequence (b_n) converges exponentially to 0 with its error shrinking by a factor near $1 - \hbar^{-1} = 0.5$. In contrast, a_n converges to 1 at doubly exponential pace with its error decreasing as $a_{n+1} - 1 \approx (a_n - 1)^4/64$.

Finally, we return to the sequence (u_n) for the saturated case $\hbar = 1$. We shall prove that $u_n \to +\infty$ as $n \to \infty$, by noting that Eq. (55) reduces to

$$u_{n+1} = u_n\left(1 + \frac{1}{u_n^2} + \frac{1}{u_n^2 + 1}\right) \geqslant 2. \tag{65}$$

Since the factor in parentheses is larger that one, (u_n) is a strictly increasing sequence. If it had an upper bound, it would converge to a number U satisfying $U \geqslant 2$ and $U = U[1 + U^{-2} + (U^2 + 1)^{-1}]$. This contradiction implies (u_n) diverges to infinity. When n increases sufficiently, $1 + u_n^{-2} + (1 + u_n^2)^{-1}$ is slightly larger than 1, and (u_n) diverges very slowly. In fact, for large n and u_n, Eq. (65) implies $\Delta u_n/\Delta n \approx$
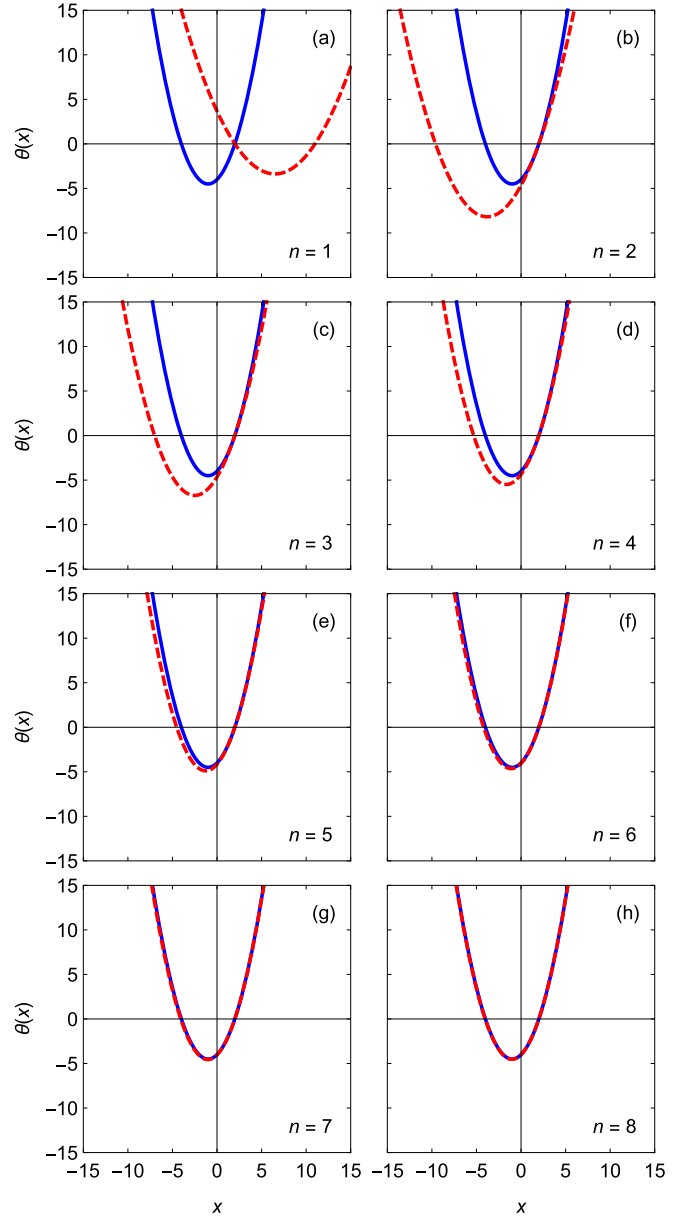

FIG. 6. Evolution of phase approximations in the position representation produced by the Gerchberg-Saxton algorithm. The Gaussian parameters are those of Fig. 1, while the initial approximation is given by $a_0 = 1/6$ and $b_0 = -3/2$. Dashed (solid) lines are for the approximations [exact solution of Fig. 2(a)].

$2/u_n$, with $\Delta n = 1$. Approximating this by a separable differential equation, and integrating we have $u_n \approx 2(n + C)^{1/2}$, where C depends solely on u_0.

As a result, (a_n) converges to zero as $0.5\sigma_k^2(n + C)^{-1/2}$, while b_n converges to k_0 with its error diminishing at an approximate ratio of $0.25/(n + C)$. This makes the parabola to straighten, over a fixed finite window, approximating the exact straight-line profile. Six snapshots of this process are displayed in Fig. 8. The Gaussian parameters of the Pauli problem are $x_0 = 2$, $\sigma_x = 1/2$, $k_0 = 3$, and $\sigma_k = 1$, thus $\hbar = 1$. The initial approximation is given by $a_0 = 1/6$ and $b_0 = -3/2$. Slow convergence as given by $a_n \approx 0.5(n + C)^{-1/2}$, with $C \approx 9.384$, is observed. It takes roughly 500
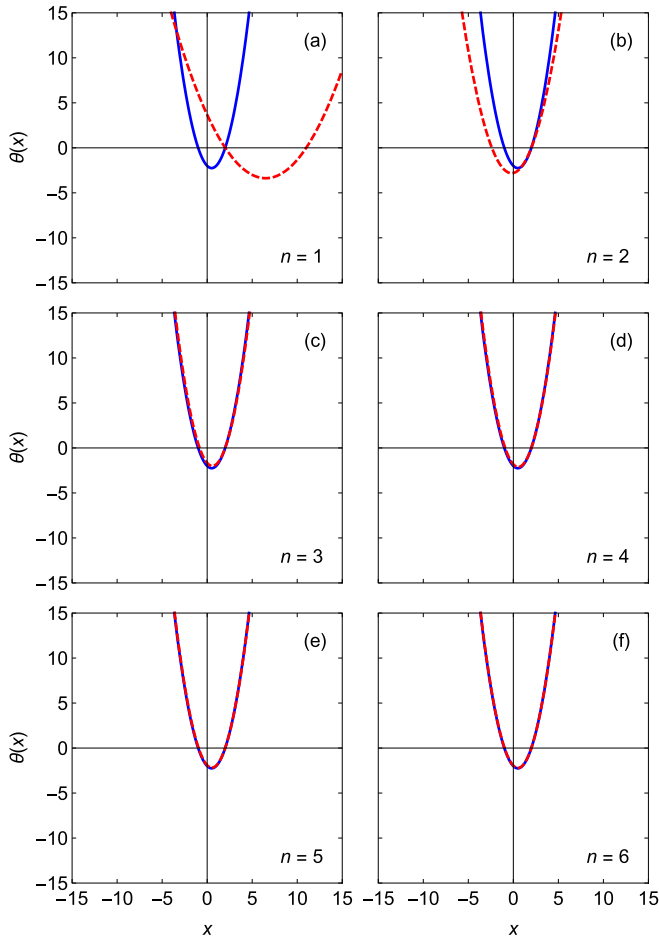
FIG. 7. As of Fig. 6, but for Gaussian parameters $x_0 = 2$, $\sigma_x = 1/2$, $k_0 = 3$, and $\sigma_k = \sqrt{2}$.

iterations to visually fit the exact solution in the selected window. Instead, when the initial approximation is a straight line, the GSA reaches the exact solution in a single iteration.

Convergence of the sequences (a_n) and (b_n) is inherited by the wave function itself. To see this, one can choose the integrated squared error

$$\epsilon_n = \int_{-\infty}^{+\infty} |\psi_n(x) - \psi(x)|^2 \, dx, \tag{66}$$

where $\psi_n(x)$ and $\psi(x)$ stand for the nth approximate and the exact wave functions, respectively. Considering the normalization condition, this leads to

$$\epsilon_n = 2\left[1 - \mathrm{Re}\left(\int_{-\infty}^{+\infty} \psi^*(x)\psi_n(x) \, dx \right) \right], \tag{67}$$

where, according to Eq. (11), the inner product reads

$$
\int_{-\infty}^{+\infty} \psi^*(x)\psi_n(x) \, dx
$$

$$
= \frac{1}{\sqrt{2\pi}\,\sigma_x} \int_{-\infty}^{+\infty} \exp\left[-\frac{(1 - iA_n)x^2}{2\sigma_x^2} + i(b_n - k_0)x \right] dx
$$

$$
= \frac{\exp\left(-\frac{B_n^2}{4(1 - iA_n)} \right)}{\sqrt{1 - iA_n}}, \tag{68}
$$

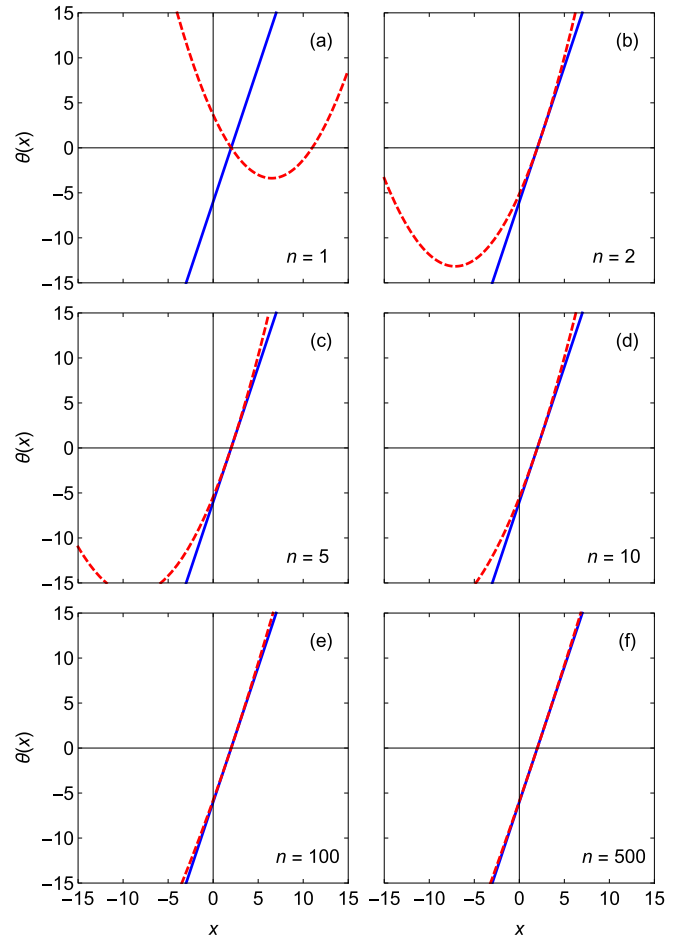with $A_n = 2\sigma_x^2(a_n - a)$ and $B_n = \sqrt{2}\sigma_x(b_n - k_0)$.

FIG. 8. As of Fig. 6, but for Gaussian parameters $x_0 = 2$, $\sigma_x = 1/2$, $k_0 = 3$, and $\sigma_k = 1$.

When n is sufficiently large, both $a_n - a$ and $b_n - k_0$ become arbitrarily small, and the integrated quadratic error can be approximated by its second-order Maclaurin expansion $\epsilon_n \approx 3\sigma_x^4(a_n - a)^2 + \sigma_x^2(b_n - k_0)^2$. If $\hbar > 1$ both terms decay exponentially. The error is dominated by the first (second) term when $\hbar < 4/3$ ($\hbar > 4/3$), so it decays exponentially as well. Instead, for $\hbar = 1$ the second term is negligible and the error decays slowly, namely $\epsilon_n \approx 3/[64(n + C)]$.

V. CONCLUSIONS

An exact retrieval of the position and momentum representations of the quantum state of a particle in one dimension has been performed. The considered Pauli problem provides Gaussian profiles for the probability densities in both representations. We distinguish two cases according to the way the Heisenberg relation between position and momentum uncertainties holds. When it is saturated, a single solution was found where the phases in position and momentum representations vary linearly. This is reinforced by the fact that saturation with given expected values and variances of position and momentum determines the quantum state uniquely [40,42]. For the harmonic oscillator of mass m, frequency ω, and characteristic length $\lambda = (m\omega/\hbar)^{-1/2}$, these minimum-uncertainty wave packets are classified as either coherent or

squeezed states, depending on whether σ_x/λ and $\sigma_k\lambda$ are equal or not, respectively. Without saturation, two linearly independent solutions (Pauli partners) were found, where the phases display parabolic profiles with opposite concavities. The partner with positive (negative) concavity is expanding (shrinking) in the position representation. Changes in the momentum uncertainty depend on the interaction potential. For the same oscillator, the Pauli partners evolve as Gaussian wave packets [36] that change expected values and uncertainties in different ways. In such a case, expansion in one representation means contraction in the other one. In fact, the sum of the squared dimensionless uncertainties in position and momentum $(\sigma_x/\lambda)^2 + (\sigma_k\lambda)^2$ is a constant of motion for Gaussian wave packets of the harmonic oscillator [37].

The exact solutions have been used to investigate the convergence of the Gerchberg-Saxton algorithm. This was done analytically, by taking a parabolic or a straight-line profile as an initial approximation for the phase in the position representation. When the Heisenberg relation is saturated, an initial parabolic profile was seen to slowly converge to a straight line. In contrast, an initial straight profile leads to an exact phase retrieval in a single iteration. When the Heisenberg relation is not saturated, the phase slope at the Gaussian center, the second derivative, and the wave function itself were shown to converge exponentially. There is a special value of the product of position and momentum uncertainties where the second derivative converges double exponentially.

More than 86 years after Pauli posed the phase-retrieval problem, a general solution has not been reported. We have given exact solutions for a particular case of broad interest. This should help tackle the problem more thoroughly. First, the role played by the uncertainty relation was discussed, showing that Pauli partners can differ in how the uncertainties evolve. Second, it should motivate the search for pairs of probability densities that allow for exact solutions of the Pauli problem. The cases with both densities being products of a Gaussian function with either a squared polynomial or a squared sinusoidal function of a second-degree polynomial deserve attention. The possibility of associating the given densities to superpositions of the same number of Gaussian wave packets should be considered as well. Two- and three-dimensional versions of the problem should lead to similar solutions but with new qualitative differences between the partners. Third, it will hopefully revive the quest of mathematicians on whether the general Pauli problem is exactly solvable. The efforts should be relevant for quantum tomography and quantum-information technologies.

Additionally, our analysis of the Gerchberg-Saxton algorithm should aid test cases in the development of numerical codes. The latter kind of approach is still needed for non-Gaussian probability densities or when the algorithm is started with a curved nonparabolic phase profile in the Gaussian case. Numerical work should help answering the question on whether the particular problem treated here allows for additional Pauli partners. More broadly, while beautiful closed form solutions are relentlessly sought for, numerical approaches will remain ubiquitous valuable tools in theoretical physics.

[1] W. Pauli, *Quantentheorie. Handbuch der Physik* (Springer, Berlin, 1933), Chap. 2.

[2] S. Weigert, Pauli problem for a spin of arbitrary length: A simple method to determine its wave function, Phys. Rev. A **45**, 7688 (1992).

[3] S. Weigert, How to determine a quantum state by measurements: The Pauli problem for a particle with arbitrary potential, Phys. Rev. A **53**, 2078 (1996).

[4] P. A. Belousov and R. S. Ismagilov, Pauli problem and related mathematical problems, Theor. Math. Phys. **157**, 1365 (2008).

[5] D. M. Goyeneche and A. C. de la Torre, State determination: An iterative algorithm, Phys. Rev. A **77**, 042116 (2008).

[6] S. Shkarin, On Pauli pairs, J. Math. Phys. **54**, 032102 (2013).

[7] W. Stulpe and M. Singer, Some remarks on the determination of quantum states by measurements, Found. Phys. Lett. **3**, 153 (1990).

[8] C. N. Friedman, Some remarks on Pauli data in quantum mechanics, J. Austral. Math. Soc. Ser. B **30**, 298 (1989).

[9] J. Corbett, The Pauli problem, state reconstruction and quantum-real numbers, Rep. Math. Phys. **57**, 53 (2006).

[10] P. Jaming, Uniqueness results in an extension of Pauli's phase retrieval problem, Appl. Comput. Harmon. A **37**, 413 (2014).

[11] A. Orłowski and H. Paul, Phase retrieval in quantum mechanics, Phys. Rev. A **50**, R921 (1994).

[12] P. Memmolo, L. Miccio, F. Merola, A. Paciello, V. Embrione, S. Fusco, P. Ferraro, and P. A. Netti, Investigation on specific solutions of Gerchberg-Saxton algorithm, Opt. Lasers Eng. **52**, 206 (2014).

[13] B. A. Shenoy, S. Mulleti, and C. S. Seelamantula, Exact phase retrieval in principal shift-invariant spaces, IEEE Trans. Signal Process. **64**, 406 (2016).

[14] G.-Z. Yang, B.-Z. Dong, B.-Y. Gu, J.-Y. Zhuang, and O. K. Ersoy, Gerchberg-Saxton and Yang-Gu algorithms for phase retrieval in a nonunitary transform system: A comparison, Appl. Opt. **33**, 209 (1994).

[15] Z. Hradil, J. Summhammer, G. Badurek, and H. Rauch, Reconstruction of the spin state, Phys. Rev. A **62**, 014101 (2000).

[16] K. Banaszek, M. Cramer, and D. Gross, Focus on quantum tomography, New J. Phys. **15**, 125020 (2013).

[17] A. Melkani, C. Gneiting, and F. Nori, Eigenstate extraction with neural-network tomography, Phys. Rev. A **102**, 022412 (2020).

[18] T. Xin, S. Lu, N. Cao, G. Anikeeva, D. Lu, J. Li, G. Long, and B. Zeng, Local-measurement-based quantum state tomography via neural networks, npj Quantum Inf. **5**, 109 (2019).

[19] A. M. Palmieri, E. Kovlakov, F. Bianchi, D. Yudin, S. Straupe, J. D. Biamonte, and S. Kulik, Experimental neural network enhanced quantum tomography, npj Quantum Inf. **6**, 20 (2020).

[20] Y. Deville and A. Deville, Quantum process tomography with unknown single-preparation input states: Concepts and application to the qubit pair with internal exchange coupling, Phys. Rev. A **101**, 042332 (2020).

[21] R. W. Gerchberg and W. O. Saxton, A practical algorithm for the determination of phase from image and diffraction plane pictures, Optik **35**, 237 (1972).

[22] J. R. Fienup, Phase retrieval algorithms: A personal tour [Invited], Appl. Opt. **52**, 45 (2013).

[23] T. Iwai and H. Masui, Application of the phase retrieval method to the refractive-index profiling of an optical fiber, Opt. Commun. **72**, 195 (1989).

[24] A. Rundquist, A. Efimov, and D. H. Reitze, Pulse shaping with the Gerchberg–Saxton algorithm, J. Opt. Soc. Am. B **19**, 2468 (2002).

[25] W. Chen, 3D Gerchberg-Saxton optical correlation, IEEE Photonics J. **10**, 7800409 (2018).

[26] P. Sun, S. Chang, S. Liu, X. Tao, C. Wang, and Z. Zheng, Holographic near-eye display system based on double-convergence light Gerchberg-Saxton algorithm, Opt. Express **26**, 10140 (2018).

[27] H. Paul, P. Törmä, T. Kiss, and I. Jex, Multiple coincidences and the quantum state reconstruction problem, Phys. Rev. A **56**, 4076 (1997).

[28] L. Liberman, Y. Israel, E. Poem, and Y. Silberberg, Quantum enhanced phase retrieval, Optica **3**, 193 (2016).

[29] C.-F. Cheng, D.-L. Liu, and D.-P. Qi, Light scattering microscopy of surface and its computational simulation, Chin. Phys. Lett. **16**, 397 (1999).

[30] R. Amézquita-Orozco and Y. Mejía-Barbosa, Gerchberg-Saxton algorithm applied to a translational-variant optical setup, Opt. Express **21**, 19128 (2013).

[31] D. S. Moore, S. D. McGrane, M. T. Greenfield, R. J. Scharff, and R. E. Chalmers, Use of the Gerchberg-Saxton algorithm in optimal coherent anti-Stokes Raman spectroscopy, Anal. Bioanal. Chem. **402**, 423 (2012).

[32] J. R. Fienup, Phase retrieval algorithms: A comparison, Appl. Opt. **21**, 2758 (1982).

[33] H. Huang, S. Yang, and R. Ye, Image encryption scheme combining a modified Gerchberg-Saxton algorithm with hyperchaotic system, Soft Comput. **23**, 7045 (2019).

[34] P. Netrapalli, P. Jain, and S. Sanghavi, Phase retrieval using alternating minimization, IEEE Trans. Signal Process. **63**, 4814 (2015).

[35] D. V. Naumov, On the theory of wave packets, Phys. Part. Nucl. Lett. **10**, 642 (2013).

[36] E. J. Heller, Time-dependent approach to semiclassical dynamics, J. Chem. Phys. **62**, 1544 (1975).

[37] M. Kleber, Exact solutions for time-dependent phenomena in quantum mechanics, Phys. Rep. **236**, 331 (1994).

[38] B. Z. Moroz and A. M. Perelomov, On a problem posed by Pauli, Theor. Math. Phys. **101**, 1200 (1994).

[39] I. S. Gradshteyn and I. M. Ryzhik, *Table of Integrals, Series, and Products*, 7th ed. (Elsevier/Academic, Amsterdam, 2007).

[40] E. Merzbacher, *Quantum Mechanics*, 2nd ed. (Wiley, New York, 1970).

[41] A. V. Aho and N. J. A. Sloane, Some doubly exponential sequences, Fibonacci Quarterly **11**, 429 (1973).

[42] J. Hilgevoord and J. Uffink, A new view on the uncertainty principle, in *Sixty-Two Years of Uncertainty*, NATO ASI Series (Series B: Physics), Vol. 225, edited by A. Miller (Springer, Boston, MA, 1990), pp. 121–137.